ChemPubSoc Europe

DOI: 10.1002/ejic.201701049

EurJIC European Journal of Inorganic Chemistry

Full Paper

Supported Catalysts

Carbon Dioxide as Feedstock in Selective Oxidation of Propane

Jungshik Kang,[a] Andrew D. Czaja,[b] and Vadim V. Guliants*[a]

Abstract: Carbon dioxide is a promising nonconventional oxidant for catalytic dehydrogenation of lower alkanes to olefins. The lower catalytic activity of CO_2 compared to oxygen, which is typically used in oxidative dehydrogenation (ODH), also means that more reactive olefins are less likely to undergo undesirable combustion in the presence of CO_2. Supported vanadia catalysts were synthesized by incipient wetness impregnation of silica supports, and by varying the surface coverage of VO_x species by means of sodium on the silica surface, the nature of the catalyst was investigated. Promotion with Na cations significantly improved the dispersion of surface VO_x species but resulted in the formation of surface Na metavanadate or another reduced V^{3+}/V^{4+} phase, which lacked catalytic activity in propane ODH in the presence of CO_2.

Introduction

Carbon dioxide (CO_2) and C_2–C_3 alkanes are well-known greenhouse gases that are generated by human activities. Our planet is projected to undergo significant environmental changes this century with potentially devastating consequences for the global economy and the natural world if humanity fails to reduce CO_2 emissions from burning fossil fuels. Electricity and heat generation combined with the use of hydrocarbon-based fuels in transportation have been the largest contributors of CO_2, creating almost two-thirds of global emissions (e.g., 5271 million tonnes of the total U.S. energy-related CO_2 emissions in 2015).[1] On the other hand, natural gas production continues to increase, as shale gas is rapidly becoming an alternative source of natural gas, and its production is currently one of the fastest growing segments of the U.S. oil and gas industry.[2] While C_2–C_3 alkanes are the major components of shale gas, they currently have no significant applications as chemical feedstocks due to their high chemical stability and the lack of technologies that can transform them selectively into chemical intermediates. Therefore, it is highly desirable to develop chemical processes that can jointly employ CO_2 and C_2–C_3 alkanes in chemical synthesis.[1,3] The total annual amount of CO_2 used in industry as a chemical feedstock to make urea, inorganic carbonates, pigments, methanol, and salicylic acid is approximately two orders of magnitude smaller than its annual atmospheric emissions.[4] Therefore, it is highly desirable to develop new large-scale chemical processes that utilize CO_2 to more fully explore the potential of its fixation into value-added products.

[a] *Department of Chemical and Environmental Engineering, University of Cincinnati, Cincinnati, OH 45221, USA*
E-mail: vadim.guliants@uc.edu
[b] *Department of Geology, University of Cincinnati, Cincinnati, OH 45221, USA*

Supporting information for this article is available on the WWW under https://doi.org/10.1002/ejic.201701049.

Selective oxidation of lower alkanes has been a long-standing fundamental and practical challenge, primarily due to the inertness of C–H bonds (e.g., the secondary C–H bond energy of 96 kcal mol^{-1} in propane) requiring energy-intensive conditions to achieve practical conversion and limited process selectivity due to greater reactivity of the partial oxidation products (e.g., propylene).[5,6] Recent reports indicated that CO_2 is a mild oxidant that can perform oxidative dehydrogenation (ODH) of lower alkanes (C_2–C_4) to the corresponding olefins [Equation (1)], all of which are valuable chemical intermediates.

$$C_nH_{2n+2} + CO_2 \rightarrow C_nH_{2n} + CO + H_2O \quad (1)$$

Ethane and propane ODH by CO_2 is expected to produce a 1:1 molar mixture of olefins with carbon monoxide that can be directly used in a variety of downstream chemical processes, such as copolymerization to produce valuable thermoplastic polyketones[7] and hydroformylation[8] to make a variety of aldehyde intermediates.

Supported vanadia and chromia catalysts have been identified in recent studies as the most promising catalysts for ODH of lower alkanes by CO_2.[9–15] These catalysts are typically synthesized by incipient wetness impregnation of oxide supports such as SiO_2, Al_2O_3, CeO_2, and ZrO_2 by solutions of V^V and Cr^{III} precursors, such as ammonium metavanadate (NH_4VO_3) and Cr^{III} nitrate, followed by drying and thermal activation at about 350 °C in air to produce well-dispersed, tetrahedrally coordinated molecular VO_x and CrO_x species on the surface of the oxide supports. The catalytic activity and selectivity of these supported VO_x and CrO_x catalysts in lower-alkane ODH is associated with the presence of monomeric and polymeric VO_x and CrO_x species at submonolayer surface coverage. Therefore, the catalytic behavior of these catalysts may be tuned by varying the surface coverage of VO_x and CrO_x species, the nature of the oxide support, and addition of promoter species.[9–15]

In a recent study,[15] silica-supported vanadia catalysts have been extensively investigated and found to be highly promising for propane ODH with molecular oxygen. However, the silica-

supported catalysts display significantly lower monolayer coverage of vanadia (ca. 3.3 V/nm^2) compared to other, more reactive oxide supports, such as alumina (7–9 V/nm^2). The promotion of silica with Na^+ cations resulted in significantly enhanced dispersion of monomeric vanadia species on SiO_2.[16] This effect was found to be optimal at a Na^+/V ratio of 0.2, and above this ratio the formation of sodium metavanadate resulted in the loss of catalytic activity. According to Grant et al.,[16] the Na^+ reacts with surface silanol groups to form more reactive Si–O–Na^+ anchoring sites that bond to several monomeric vanadia species. Therefore, the use of the Na^+ species to promote VO_x dispersion on the silica surface offers new opportunities to design novel 2D metal oxide catalysts supported on SiO_2. According to Grant et al.,[16] greater surface coverage of 2D vanadia species in Na-promoted catalysts leads to a higher rate of propane ODH while maintaining high propylene selectivity. However, the behavior of Na-promoted vanadia catalysts in propane ODH by CO_2 has not been investigated. Therefore, in this study we synthesized Na-promoted vanadia catalysts supported on silica and investigated their behavior in propane ODH reactions employing molecular oxygen and CO_2.

Results and Discussion

Table 1 shows the composition of model supported vanadia catalysts synthesized in this study. A series of VO_x/SiO_2 catalysts were synthesized at different vanadia loadings to study the effect of vanadia surface coverage on conversion and selectivity in propane ODH. The vanadia surface coverage[16] in these catalysts ranged from 54 to 185 % of a theoretical monolayer on the silica support in the absence of Na^+, and from 21 to 72 % for the Na-promoted silica.

Table 1. Vanadium content in silica-supported catalysts.

Samples	V [%][a]	V/nm^2	Coverage [% monolayer]	
			Silica	Na-promoted
S1 or Na-S1	4.2	1.9	54.0	21.2
S2 or Na-S2	6.9	3.1	88.0	34.4
S3 or Na-S3	9.1	4.1	117.1	45.6
S4 or Na-S4	14.7	6.6	185.7	72.2

[a] The vanadium content (wt. %) was analyzed by energy-dispersive X-ray spectroscopy (EDS).

The occurrence of homogeneous reactions was investigated first by passing the above-mentioned propane/O_2 and propane/CO_2 mixtures through an empty reactor and over the original silica support at 550–750 °C. For an empty reactor, trace amounts of ethylene and methane were detected above 650 °C for the propane/O_2 mixture, while no reaction was observed for the propane/CO_2 mixture at any temperature. Similar results were observed for the ODH reactions over the original silica support, that is, trace levels of ethylene and methane above 550 °C for the propane/O_2 mixture. Moreover, no reaction products were observed up to 700 °C for the propane/CO_2 mixture, while above 700 °C, CO and a trace amount of propane cracking products were observed. However, we observed the occurrence of homogeneous combustion reaction over silica support in the presence of O_2 above 600 °C, as well as cracking reaction products when the reactor temperature was further increased to 700 °C. However, no reactions were observed over the silica support at relevant temperatures (600 °C and below) employed in this study to investigate propane ODH reactions. Moreover, while propane ODH in the presence of O_2 and CO_2 was investigated over silica-supported vanadia catalysts at 350–600 °C, significant propane conversion was observed only at 550 and 600 °C.

Table 2 shows the initial propane conversion and product selectivity of propane ODH over VO_x/SiO_2 catalysts at 550 °C. In the case of O_2, the formation of C_1 and C_2 products increased with increasing vanadia content in these catalysts. Also, as expected, the conversion of propane was considerably higher during O_2 ODH compared to CO_2 ODH. However, the propylene yield was similar for both CO_2 and O_2 ODH reactions due to a greater extent of cracking reactions during O_2 ODH. The propane conversion over S1 catalyst (1.9 V/nm^2) was 18 mol-% for O_2 ODH and 9.2 mol-% for CO_2 ODH, while it increased with vanadia content, for example, to 25 mol-% for the S2 catalyst for both O_2 and CO_2 ODH reactions, and reached a maximum for the S3 catalyst. The maximum yield of propylene of about 11 mol-% was observed over S2 catalyst (3.1 V/nm^2). Note that the S1 catalyst corresponded to about 50 % of theoretical monolayer coverage of vanadia on silica, whereas the S2 and S3 catalysts are characterized by about 90 and 120 % monolayer coverage, respectively. Therefore, on the basis of the initial reactivity of VO_x/SiO_2 catalysts in these two ODH reactions, one may conclude that the presence of a monolayer of surface VO_x species is important for the reactivity in these propane ODH reactions.

Table 2. Propane ODH reactions over VO_x/SiO_2 catalysts at 550 °C.[a]

V/nm^2	Oxidant	C_3H_8 conv. [%]	Coverage [% monolayer]					Yield [%]
			CO	CO_2	CH_4	C_2H_4	C_3H_6	
1.9	O_2	18.7	28.1	15.6	16.4	0.0	39.3	
(S1)	CO_2	9.2	60.6	–	0.0	0.0	39.4	7.4
3.1	O_2	27.3	26.4	0.0	32.0	0.0	41.6	3.6
(S2)	CO_2	25.0	51.5	–	3.4	0.0	45.1	11.4
4.1	O_2	37.2	28.0	13.6	49.0	1.0	9.4	11.3
(S3)	CO_2	29.4	86.8	–	3.4	0.0	9.8	3.5
6.6	O_2	38.5	18.0	8.5	40.0	5.3	28.0	2.9
(S4)	CO_2	22.3	77.6	–	0.0	0.0	22.4	10.8

[a] Reaction conditions: 550 °C, gas hourly space velocity (GHSV) = 2500 h^{-1}, O_2/C_3H_8 = 1:2, CO_2/C_3H_8 = 2:1, He balance.

Table 3 shows the initial propane conversions and product selectivities for propane ODH over VO_x/SiO_2 catalysts at 600 °C. The propane conversion and formation of C_1–C_3 cracking products increased dramatically at 600 °C, while the propylene yield was not significantly affected. The main difference in reaction products observed for CO_2 and O_2 ODH reactions was the significant amount of CO produced in the former case and methane in the latter. The C_2 products ethane and ethylene were not observed among the reaction products during CO_2 ODH, except over the S4 catalyst (6.6 V/nm^2) at 600 °C, which contained about 180 % theoretical monolayers of VO_x species. However, ethylene and CO_2 were already observed at low temperature (450 °C) during O_2 ODH. The conversion of propane

increased with increasing VO_x coverage, reaching a maximum over the S3 catalyst and then declining at higher VO_x coverage.

Table 3. Propane ODH reactions over VO_x/SiO_2 catalysts at 600 °C.[a]

V/nm²	Oxidant	C_3H_8 conv.	Coverage [% monolayer]					Yield
		[%]	CO	CO_2	CH_4	C_2H_4	C_3H_6	[%]
1.9	O_2	22.9	27.7	14.6	15.5	9.5	32.9	7.5
(S1)	CO_2	13.7	50.9	–	9.0	0.0	40.2	5.5
3.1	O_2	33.4	6.8	18.8	25.0	18.9	30.4	10.1
(S2)	CO_2	29.2	69.0	–	9.7	0.0	21.4	6.3
4.1	O_2	52.1	28.0	10.3	47.0	4.8	10.3	5.4
(S3)	CO_2	50.7	84.7	–	4.0	0.0	11.3	5.7
6.6	O_2	45.9	23.8	14.9	39.0	7.0	15.0	6.9
(S4)	CO_2	31.1	71.7	–	13.2	2.5	12.6	3.9

[a] Reaction conditions: 600 °C, GHSV = 2500 h^{-1}, O_2/C_3H_8 = 1:2, CO_2/C_3H_8 = 2:1, He balance.

Turnover frequencies (TOF) for propane consumption were calculated by Equation (2):

$$TOF = \frac{\dot{n}_{C_3H_8,0} \cdot X_{C_3H_8} \cdot M_V}{m_{cat} \cdot w_v \cdot 10^{-2}} \quad (2)$$

The TOFs report the numbers of propane molecules converted at each VO_x species per second, where $\dot{n}$ denotes the molar flow rate of propane [mol/s], X the fractional conversion, M_V the molar mass of vanadium [g/mol], m_{cat} the catalyst weight [g], and W_V the vanadium content [wt. %]. Figure 1 shows the TOFs for propane consumption as a function of surface VO_x coverage at 500 °C at different space velocities to maintain low propane conversion (<15 %). All supported vanadia catalysts showed very similar TOFs, except for the S1 catalyst (lowest V content). The S2 and S3 catalysts (3.1 and 4.1 V/nm², respectively, close to theoretical monolayer coverage) showed the maximum TOF, but the values only varied from 3.8×10^{-3} s^{-1} to 4.1×10^{-3} s^{-1} among the three vanadia catalysts S2, S3, and S4.

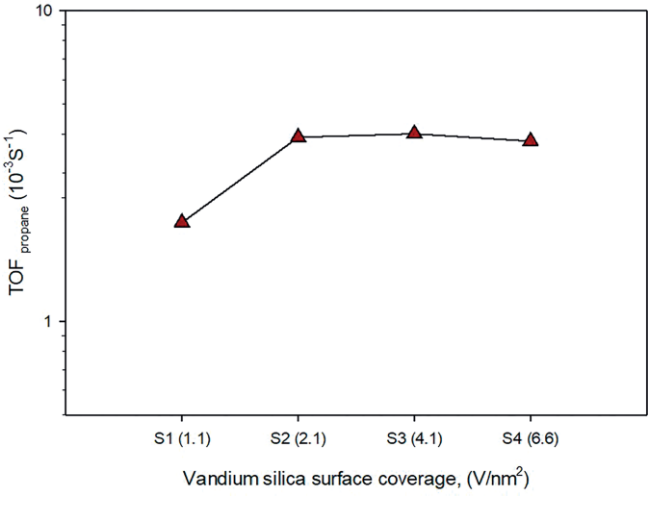

Figure 1. Propane-consumption TOFs as a function of surface VO_x coverage at 500 °C, determined at a propane conversion of about 15 %.

All supported vanadia catalysts were further investigated at 550 and 600 °C, GHSV = 2500 h^{-1}, and feed composition of CO_2/C_3H_8 = 2:1 (Figures S1–S4) as a function of time on stream. The S1 catalyst (1.9 V/nm²) initially displayed low catalytic activity at 550 °C, which was subsequently lost after 2 h under catalytic reaction conditions, while stable catalytic behavior was observed at 600 °C for more than 3.5 h. The S2 catalyst (3.1 V/nm²) initially showed high catalytic activity, which continuously declined with time at 550 °C. The formation of C_1 and C_2 products dramatically increased at 600 °C after 3 h on stream, while propane conversion and propylene selectivity decreased. On the other hand, the catalytic activity rapidly decreased over the S3 catalyst (4.1 V/nm²) with time on stream. These results indicated that the VO_x/SiO_2 catalysts are rapidly deactivated with increasing VO_x content above the theoretical monolayer coverage. The catalytic activity did not increase with reaction temperature, while the selectivity to propylene decreased at the expense of propane cracking reactions. Moreover, the S2 and S3 catalysts that showed higher conversion for CO_2 ODH of propane tended to be deactivated rather quickly with time on stream. Also, deactivation of the S2 and S3 catalysts was accelerated at a higher reaction temperature of 600 °C, as propane conversion decreased by about 50 % after 1 h under catalytic reaction conditions. These results suggested that a more limited extent of surface reoxidation with increased VO_x coverage may be responsible for the decreased ODH activity of VO_x/SiO_2 catalysts.

Figure 2 shows the thermogravimetric analysis (TGA) curves for used VO_x/SiO_2 catalysts after CO_2 ODH of propane at 600 °C for 72 h. All used catalysts exhibited a weight losses during TGA in air associated with carbon deposition, whereas used catalysts after O_2 ODH showed very little weight loss features in TGA. Recently, Ascoop et al.[17] also reported significant carbon deposition even after a short time on stream during CO_2 ODH of propane over VO_x/SiO_2 catalysts. The extent of carbon deposition varied with varying vanadium content, and two catalysts with near-monolayer coverage, that is, S2 (3.1 V/nm²) and S3 (4.1 V/nm²), showed much higher weight losses of about 45 and 20 wt.-%, respectively, while S1 (1.9 V/nm², ca. 0.5 monolayers) showed almost no weight loss during TGA. These observed differences in carbon deposition behavior may be related to cata-

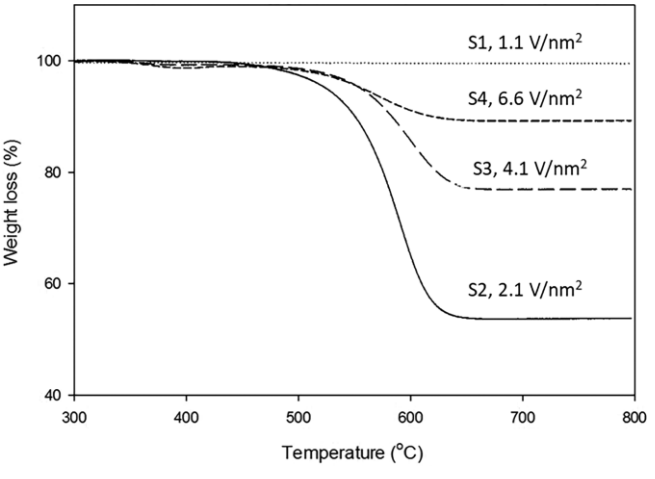

Figure 2. TGA curves in air for VO_x/SiO_2 catalysts after CO_2 ODH of propane at 600 °C for 72 h.

lytic activity, since the catalysts showing higher reactivity in CO_2 ODH of propane displayed greater carbon deposition. These results suggested that the acidic silica support may also play a role in initiating carbon deposition by adsorbing hydrocarbon intermediates during the ODH reaction in the presence of CO_2. However, the exposure of the silica surface to hydrocarbon intermediates is minimized above monolayer coverage of the VO_x species, for example, for S4 (6.6 V/nm^2), and this explains the diminished carbon deposition observed for this catalyst (ca. 2 % weight loss).

Na-promoted silica supports were employed to improve surface dispersion of 2D VO_x species. Table 4 shows the results of CO_2 ODH of propane over Na-promoted VO_x/SiO_2 catalysts prepared at the same VO_x surface coverage as the Na-free supported VO_x catalysts (Table 1). Unlike Na-free catalysts, Na-promoted VO_x/SiO_2 catalysts showed no selectivity to propylene and instead displayed increasing tendency to form cracking products, ethane and methane, with increasing vanadium content. The Na-promoted catalysts showed very low catalytic activity at 550 and 600 °C. At a high reaction temperature of 600 °C, a selectivity of greater than 85 % to ethylene was observed over all the catalysts, while at a reaction temperature of 550 °C only CO was observed with very low propane conversion of less than 2 %. The selectivity to C_2 species (ethane and ethylene) was particularly high and remained relatively constant over all catalysts investigated, and this suggests that these species may represent reaction intermediates during propane/propylene degradation to methane.

Table 4. Results of CO_2 ODH of propane over sodium-promoted silica catalysts with various vanadium contents.[a]

Samples	*T* [°C]	C_3H_8 conv. [%]	Selectivity [%] CO	CH_4	C_2H_4	C_3H_6
1.9	550	1.3	100	0.0	0.0	0.0
(Na-S1)	600	3.4	6.3	8.2	85.5	0.0
3.1	550	0.9	100	0.0	0.00	0.0
(Na-S2)	600	2.2	5.5	8.3	86.2	0.0
4.1	550	0.9	100	0.0	0.00	0.0
(Na-S3)	600	4.3	6.3	8.3	85. 5	0.0
6.6	550	1.8	100	0.0	0.0	0.0
(Na-S4)	600	5.5	4.0	8.0	88.0	0.0

[a] Reaction conditions; GHSV = 2500 h^{-1}, O_2/C_3H_8 = 1:2, CO_2/C_3H_8 = 2:1, He balance.

Raman spectra of the Na-free and Na-promoted silica support and VO_x/SiO_2 catalysts were recorded to establish the nature of the surface species in these two series of supported vanadia catalysts. Figure 3 shows the Raman spectra of the Na-free and Na-promoted silica supports. Raman peaks at 1058 and 1023 cm^{-1} in the spectrum of the Na-bearing silica support (upper spectrum in Figure 3) are assigned to sodium silicate.[16] Figure 4 shows the Raman spectra of Na-free and Na-promoted S2 catalysts as well as corresponding silica supports. The Raman spectrum of the Na-free S2 catalyst (upper spectrum in Figure 4a) shows peaks at 993 and 1033 cm^{-1}, which correspond to the bulk V_2O_5 crystals and V=O stretching vibration of the monomeric VO_x species, respectively.[17] The addition of Na resulted in the appearance of Raman peaks at 506, 637, 914, and 950 cm^{-1} associated with the presence of Na metavanadate instead of 2D or 3D vanadia.[18] Sodium metavanadate was previously reported to be inactive in ODH reactions,[16–19] which may explain the lack of catalytic activity of our Na-promoted VO_x/SiO_2 catalysts. According to Irusta et al.,[19] vanadate spe-

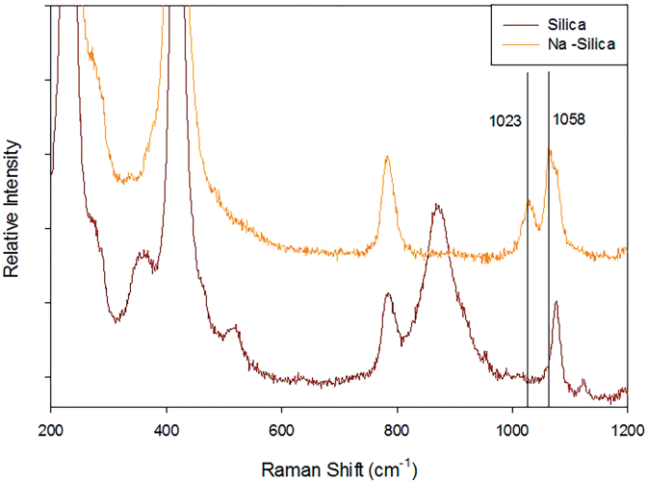

Figure 3. Raman spectra of the original and Na-promoted silica support.

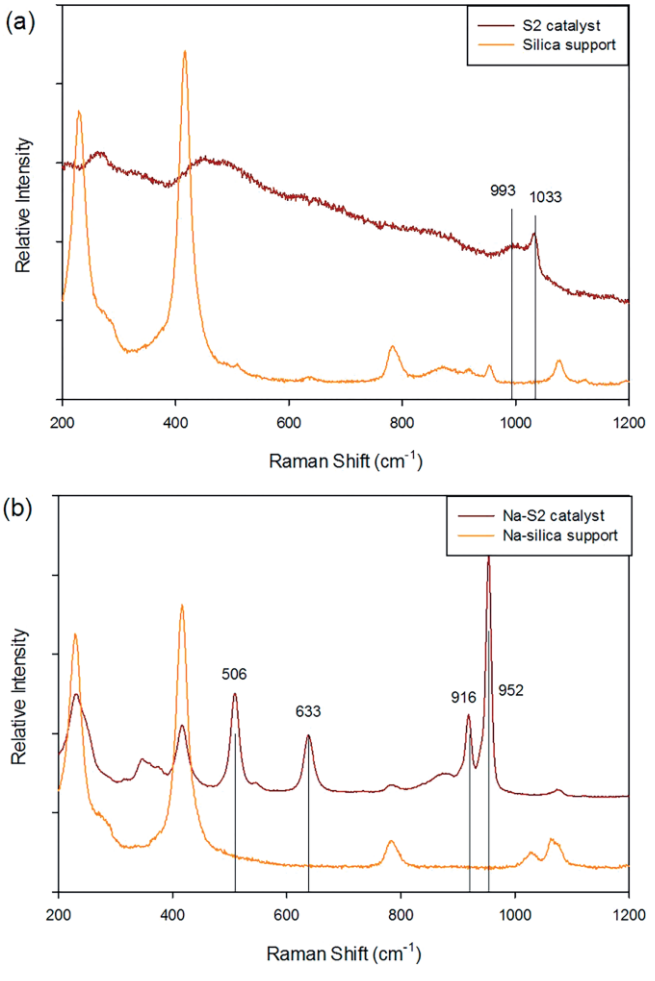

Figure 4. Raman spectra of Na-free (top) and Na-promoted (bottom) S2 catalyst (3.1 V/nm^2) as well as corresponding silica supports.

cies react with Na^+ cations present on the surface of the Na-promoted silica to form surface $NaVO_3$-like compounds that are inactive for methane oxidation to formaldehyde. Similar observations were made by Adamski et al.,[20] who reported that the conversion of propane during its ODH over alkali metal doped supported 3V/Zr catalysts decreased in the following order: undoped > Li^+ > Na^+ > K^+, indicating that alkali metal dopants were detrimental to the ODH activity of supported vanadia catalysts. Furthermore, we confirmed carbon deposition in used catalysts by comparing the Raman spectra of fresh and used catalysts. Figure 5 compares the Raman spectra of fresh and used S4 catalysts after propane ODH in the presence of CO_2 (GHSV = 2500 h^{-1} and CO_2/C_3H_8 = 2:1 in He balance at 600 °C). The Raman peaks at 993 and 1033 cm^{-1} decreased in intensity due to reduction of VO_x species during the reaction, which represent the stretching mode of monomeric V=O species, while new peaks were observed at 1350 and 1598 cm^{-1} that correspond to the D and G bands of carbon. The G band represents graphitic carbon and the D band represents disorder of the sp^2-bonded carbon.[21]

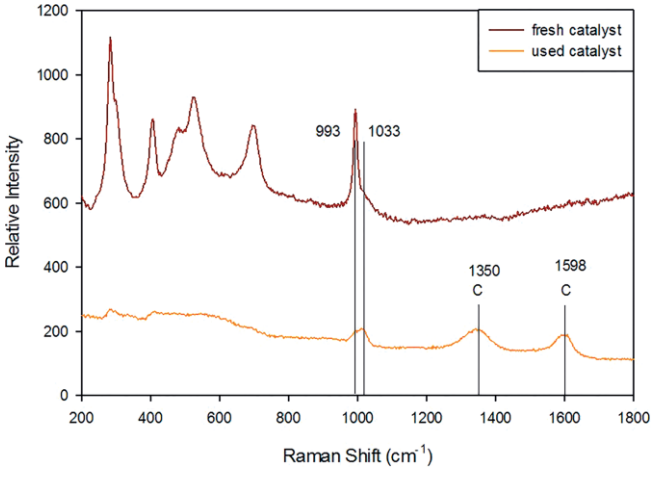

Figure 5. Raman spectra of fresh and used S4 catalysts after propane ODH in the presence of CO_2 (GHSV = 2500 h^{-1}, CO_2/C_3H_8 = 2:1, He balance at 600 °C).

Figure 6 shows the Raman spectra of the Na-free and Na-promoted S4 catalysts containing the highest VO_x loading (6.6 V/nm^2). The V=O stretching band that is clearly observed at 1028 cm^{-1} in the absence of Na^+ indicates the presence of molecularly dispersed VO_x species. However, broadening of this band with increasing vanadium content might be due to a higher content of microcrystalline V_2O_5 compared to the catalysts with lower VO_x coverage. The Raman features of molecularly dispersed VO_x species were absent in the Raman spectrum of the Na-promoted S4 catalyst. Surface Na metavanadate was also expected for this catalyst, although its Raman spectrum lacked strong features associated with Na metavanadate, in agreement with previous observations.[16] Improved vanadium dispersion in the presence of Na^+ was further confirmed by EDS elemental mapping. Figure S5 shows the results of elemental mapping for V, Si, O, C, and Na on Na-free and Na-promoted S4 catalysts (6.6 V/nm^2) corresponding to the highest V loading investigated in this study. In the absence of Na^+, a large vanadium oxide particle is visible in the center top region of the images shown in Figure S5a, which confirms that VO_x species form a bulk phase above theoretical monolayer coverage (185.7 % in Table 1). In the presence of Na^+, the dispersion of VO_x species is improved significantly, as manifested in the absence of large vanadium oxide particles (Figure S5b). Increased theoretical monolayer coverage of VO_x in Na-promoted catalysts reduces the V surface coverage in the Na-promoted S4 catalyst to about 72.2 % of the theoretical monolayer (Table 1). However, while Na promotion improves the dispersion of VO_x species on silica, it results in the formation of surface Na metavanadate species that lack catalytic activity in both propane ODH reactions. The presence of Na^+ is believed to adversely affect the redox behavior of surface VO_x species, which prevents the regeneration of the V^{5+} oxidation state important for propane activation.

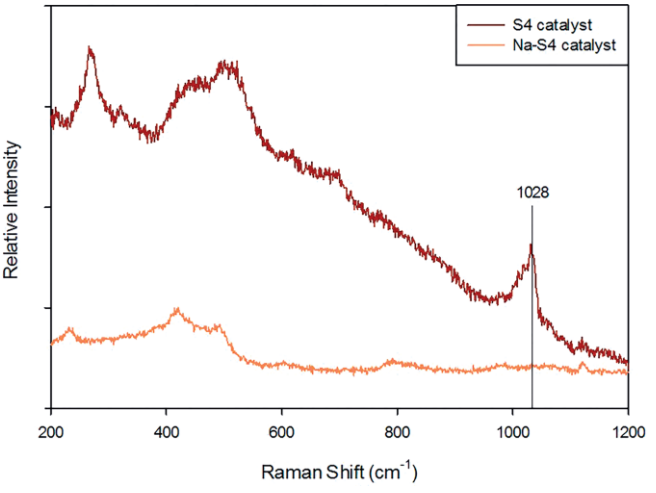

Figure 6. Raman spectra of the Na-free and Na-promoted S4 catalyst (6.6 V/nm^2).

Conclusions

Propane ODH by O_2 and CO_2 was performed over Na-free and Na-promoted supported VO_x/SiO_2 catalysts. The propylene yield was very similar in both CO_2 and O_2 ODH reactions with a maximum value of about 11 mol-% observed for the S2 catalyst. However, the propane conversion increased dramatically with increasing vanadium content, for example, 18 % for O_2 and 9.2 % for CO_2 ODH at 1.9 V/nm^2 for the S1 catalyst, while it increased to greater than 25 % at higher VO_x loadings for both O_2 and CO_2 ODH. We observed a trend through Raman spectroscopic studies that with increasing vanadium content on silica, 2D vanadia structures are formed at first, and then formation of 3D vanadia crystalline structure is favorable. Thus, the maximum amount of 2D vanadia structure that shows high activity for CO_2 ODH of propane was obtained in a monolayer-coverage range, and we confirmed this by calculating the TOF of propane conversion. Considerable carbon deposition was observed in used catalysts after propane ODH by CO_2, the extent of which correlated with their catalytic activity. Promotion with Na cations significantly improved the dispersion of surface VO_x species and resulted in the formation of surface Na metavana-

date or another reduced V^{3+}/V^{4+} phase, which displayed no catalytic activity in propane ODH in the presence of CO_2.

Experimental Section

A series of VO_x/SiO_2 catalysts were synthesized with different vanadia loadings to study the effect of vanadia surface coverage on conversion and selectivity in propane ODH. Ammonium metavanadate (Sigma-Aldrich, 99 % ACS grade) was deposited on a commercial silica support (Saint-Gobain, SS 61138, BET surface area: 261 $m^2\,g^{-1}$) by incipient wetness impregnation at four different vanadia loadings. After impregnation, the as-synthesized catalysts were dried in a vacuum oven at 60 °C for 4 h and then calcined in air at 550 °C for 3 h. , Four different Na-promoted VO_x/SiO_2 catalysts were also synthesized with the same vanadia loadings (Table 1). First, Na-promoted silica supports were prepared by incipient wetness impregnation of the same silica support with a solution of $NaNO_3$ (Fisher Scientific, Certified ACS Grade, >99 % purity). Na loadings were adjusted for different supported vanadia catalysts to yield Na-promoted VO_x/SiO_2 catalysts with an atomic ratio of Na/V = 0–0.3. Prior to VO_x deposition, as-synthesized Na-promoted silica was calcined in air by ramping the temperature at 1.5 °C min^{-1} to 700 °C and holding for 4 h. These catalysts were then synthesized by the same procedures as described above for the Na-free catalysts. The surface loadings (V/nm^2) and coverages (% of the theoretical monolayer) reported in Table 1 were calculated on the basis of EDS V and Si compositions in these catalysts. The V content (wt. %) was converted to surface loadings (V/nm^2) according to Equation (3):

$$\frac{V}{nm^2} = \frac{V(wt.\%)\cdot N_A\left(\frac{atoms}{mol}\right)}{100\left(\frac{g}{g}\right)\cdot AW_V\left(\frac{g}{mol}\right)\cdot S_{BET}\left(\frac{m^2}{g}\right)\cdot 10^{18}\left(\frac{nm^2}{m^2}\right)} \quad (3)$$

These loadings were referenced to theoretical monolayer coverages reported by Grant et al.[16] to yield the vanadium surface coverages reported in Table 1.

Oxidative dehydrogenation of propane by O_2 and CO_2 was performed at atmospheric pressure in a continuous-flow fixed-bed tubular reactor. Different VO_x/SiO_2 catalysts (0.5 g) placed between quartz wool plugs inside the reactor (a stainless steel tube of 1/4 inch O.D.) were pretreated in a flowing O_2/He mixture (10 mL/min each) for 1 h at 450 °C prior to the catalytic tests. The feed gas mixture consisted of helium (UHP grade, Wright Brothers, Inc.), carbon dioxide (Tech. grade, Wright Brothers, Inc.) or oxygen (UHP grade, Wright Brothers, Inc.), and propane (CP grade, Matheson gas) at a total flow rate of 16 mL/min to establish a GHSV of 2500 h^{-1}. The O_2 concentration employed in these studies was half of the CO_2 concentration used in ODH reaction to minimize homogeneous oxidation of propane (propane/oxidant ratio of 2:1 for CO_2 and 1:1 for O_2, balance of He), while the reaction temperature was varied from 350 to 550 °C. The effluent gas was directly passed through heated sampling valves to an online GC–MS system (Shimadzu, GC–MS QP-5000) equipped with a capillary column (Supelco, Carboxen 1006 PLOT, fused silica) of 30 m in length and 0.32 μm film thickness with ultrapure helium (Wright Brother Inc., Lot 9047–1) as the carrier gas. The products were identified by using NIST Mass Spectrum Library 2008 (Shimadzu, No. 225-13290-91). The catalysts were also characterized by TGA (SDT-Q600 unit from TA Instruments, New Castle, DE, USA) and Raman spectroscopy (Horiba T64000, Horiba Scientific, Edison, NJ, USA) with a 514 nm laser line, before and after the ODH of propane. STEM imaging and EDS elemental mapping of the two S4 catalysts corresponding to the highest V surface loading investigated in this study were conducted using the FEI Probe Corrected Titan3™ 80–300 S/TEM.

Acknowledgments

This research was supported by the Ohio Coal Development Office under grant no. OCDO R-12-14.

Keywords: Supported catalysts · Vanadium · Oxidation · Heterogeneous catalysis · Sodium

[1] V. Havran, M. P. Dudukovic, *Ind. Eng. Chem. Res.* **2011**, *50*, 7089–7100.
[2] The US Energy Information Administration, **2016**: http://www.eia.gov/tools/faqs/faq.cfm?id = 77&t = 11.
[3] The US Energy Information Administration's Annual Energy Outlook **2015** (AEO2015): http://www.eia.gov/forecasts/aeo/.
[4] J. N. Armor, *J. Energy Chem.* **2013**, *22*, 21–26.
[5] R. K. Grasselli, *Catal. Today* **2005**, *99*, 23–31.
[6] M. Zboray, A. T. Bell, E. Iglesia, *J. Phys. Chem. C* **2009**, *113*, 12380–12386.
[7] E. Drent, W. P. Mul, A. A. Smaardijk, *Encyclopedia of Polymer Science and Technology.* John Wiley & Sons, Inc. **2001**, https://doi.org/10.1002/0471440264.pst273.
[8] V. Leeuwen, W. N. M. Piet, C. Claver, *Rhodium Catalyzed Hydroformylation*, Springer, **2002**, https://doi.org/10.1007/0-306-46947-2.
[9] N. Mimura, M. Okamoto, H. Yamashita, S. T. Oyama, K. Murata, *J. Phys. Chem. B* **2006**, *110*, 21764–21770.
[10] M. A. Smith, A. Zoelle, Y. Yang, R. M. Rioux, N. G. Hamilton, K. Amakawa, P. K. Nielsen, A. Trunschke, *J. Catal.* **2014**, *312*, 170–178.
[11] Z. W. Liu, C. Wang, W. B. Fan, Z. T. Liu, Q. Q. Hao, X. Long, J. Lu, J. G. Wang, Z. F. Qin, D. S. Su, *ChemSusChem* **2011**, *4*, 341–345.
[12] G. Raju, B. M. Reddy, B. Abhishek, Y. H. Mo, S. E. Park, *Appl. Catal. A* **2012**, *423–424*, 168–175.
[13] W. Z. Li, F. Gao, Y. Li, E. D. Walter, J. Liu, C. H. F. Peden, Y. Wang, *J. Phys. Chem. C* **2015**, *119*, 15094–15102.
[14] V. V. Guliants, *Catal. Today* **1999**, *51*, 255–268.
[15] C. A. Carrero, R. Schloegl, I. E. Wachs, R. Schomaecker, *ACS Catal.* **2014**, *4*, 3357–3380.
[16] J. T. Grant, C. A. Carrero, A. M. Love, R. Verel, I. Hermans, *ACS Catal.* **2015**, *5*, 5787–5793.
[17] I. Ascoop, V. V. Galvita, K. Alexopoulos, M. Reyniers, P. V. D. Voort, V. Bliznuk, G. B. Marin, *J. Catal.* **2016**, *335*, 1–10.
[18] S. Seetharaman, H. L. Bhat, P. S. Narayanan, *J. Raman Spectrosc.* **1983**, *14*, 401–405.
[19] S. Irusta, A. J. Marchi, E. A. Lombardo, E. E. Miré, *Catal. Lett.* **1996**, *40*, 9–16.
[20] A. Adamski, Z. Sojka, K. Dyrek, *Langmuir* **1999**, *15*, 5733–5741.
[21] A. C. Ferrari, J. Robertson, *Phys. Rev. B* **2000**, *61*, 14095–14107.

Received: August 31, 2017